Seasonal circulation on the western shelf of the Gulf of Mexico using a high-resolution numerical model

Jorge Zavala-Hidalgo,[1] Steven L. Morey, and James J. O'Brien
Center for Ocean-Atmospheric Prediction Studies, Florida State University, Tallahassee, Florida, USA

Received 31 March 2003; revised 18 July 2003; accepted 23 September 2003; published 26 December 2003.

[1] The seasonal circulation on the western shelf of the Gulf of Mexico is studied using a high-resolution numerical simulation, historical hydrographic data, sea level data, and satellite images. Three regions are distinguished, the Tamaulipas-Veracruz (TAVE) shelf, the Louisiana-Texas (LATEX) shelf, and the western Campeche Bank. On the TAVE shelf there is a swift reversal of the along-shelf current, downcoast from September to March and upcoast from May to August when there is upwelling due to offshore Ekman transport. Circulation on the western Campeche Bank is upcoast throughout the year. The LATEX shelf has a cyclonic circulation, except during summer months when the flow is eastward. During spring-summer the upcoast current on the TAVE shelf reaches the southern Texas shelf where it encounters a downcoast coastal current favoring offshore transports. In the fall-winter, the downcoast current reaches the southern Bay of Campeche where it meets an opposing along-shelf current, generating seasonal offshore transports. During fall and winter, cool low-salinity water from the Mississippi and Atchafalaya Rivers is advected westward along the LATEX shelf onto the TAVE shelf, developing along-shelf fronts and temperature inversions commonly observed over the outer shelf and shelf break. The main forcing over the western shelf of the gulf is the along-coast wind stress component. The existence of the cross-shelf transports in the confluence regions is supported by chlorophyll *a* data. Up to 80% of the seasonal sea level variability is explained by the along shelf currents and the low-frequency variability of the atmospheric sea level pressure. *INDEX TERMS:* 4227 Oceanography: General: Diurnal, seasonal, and annual cycles; 4219 Oceanography: General: Continental shelf processes; 4223 Oceanography: General: Descriptive and regional oceanography; *KEYWORDS:* shelf circulation, western Gulf of Mexico

Citation: Zavala-Hidalgo, J., S. L. Morey, and J. J. O'Brien, Seasonal circulation on the western shelf of the Gulf of Mexico using a high-resolution numerical model, *J. Geophys. Res.*, *108*(C12), 3389, doi:10.1029/2003JC001879, 2003.

1. Introduction

[2] Considering the continental platform west of 89.5°W as the western shelf of the Gulf of Mexico (GoM), it includes the Louisiana-Texas (LATEX) shelf and the shelves of the Mexican states of Tamaulipas, Veracruz, Tabasco, Campeche, and part of Yucatan, up to Puerto Progreso. Defining the outer shelf boundary at 200 m, the western shelf has an area of 267,000 km^2 and its length, disregarding features smaller than 50 km, is around 2,500 km (Figure 1).

[3] Although the circulation on the LATEX shelf at the seasonal frequency is well known, the region is included in this study because it is found that there is a strong relation between its dynamics and that of the Mexican shelf. Its inclusion is also useful to validate the model results because the amount of data and number of studies are larger here compared to those on the Mexican shelf. On the LATEX shelf the dominant pattern is a cyclonic circulation with a wind-driven downcoast (in the direction that the Kelvin wave travels) jet near the coast and a weaker northeastward current on the outer shelf [*Cochrane and Kelly*, 1986; *Oey*, 1995; *Li et al.*, 1996; *Cho et al.*, 1998; *Nowlin et al.*, 1998]. This pattern prevails most of the year except from June to August when the surface currents run upcoast over almost the entire shelf, excluding some regions near the coast mostly on the eastern side of the shelf. The mainly wind driven nearshore flow is enhanced by the Mississippi-Atchafalaya Rivers discharge [*Li et al.*, 1997]. The concave shape of the coast and the wind stress forcing cause a convergence of currents on the western side of the LATEX shelf and a divergence on the eastern side. *Cochrane and Kelly* [1986] proposed that the convergence and divergence completes the gyre and drives the southern limb of the gyre. Alternatively, *Oey* [1995] proposed that the southern limb of the gyre may be driven by mesoscale eddies next to the shelf break, and the studies from the LATEX program [*Nowlin et al.*, 1998] showed that the outer shelf is mainly driven by the mesoscale eddies that have not annual periodicity. The convergence at the western end of the gyre migrates seasonally, reaching south of the Rio Grande

[1]Now at Centro de Ciencias de la Atmósfera, Universidad Nacional Autónoma de México, México, México.

0148-0227/03/2003JC001879$09.00

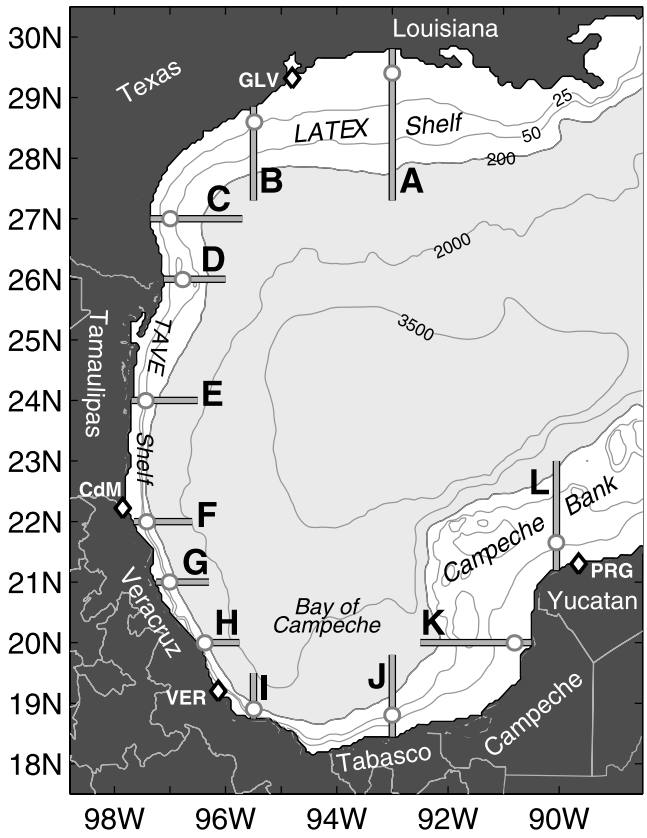

Figure 1. Location of the western Gulf of Mexico and sites of interest. Sections where detailed analysis is presented are indicated with capital letters, and circles indicate the sites (stations) of surface currents in Figure 11. Tide gauge locations are indicated: Galveston (GLV), Ciudad Madero (CdM), Veracruz (VER), and Progreso (PRG).

mouth in fall. Most of the year, along-shore isohalines prevail with lower salinity inshore, but during July and August, cross-shelf isohalines are observed with lower salinity in the east [*Cochrane and Kelly*, 1986; *Li et al.*, 1997; *Nowlin et al.*, 1998]. Interannual variability in the LATEX shelf circulation has been documented, which is particularly noticeable during the periods when the currents reverses because the current can flow in opposite directions in different years as *Cho et al.* [1998] and *Nowlin et al.* [1998] showed that happened during the period from April 1992 to November 1994.

[4] The dynamics of the shelf south of the United States-Mexican border are less known. Most of the studies in the western GoM have been dedicated to processes that occur mainly offshore from the shelf: eddies and their interaction with the slope [*Merrell and Morrison*, 1981; *Brooks and Legeckis*, 1982; *Elliott*, 1982; *Merrell and Vázquez*, 1983; *Vidal et al.*, 1994a], and the western boundary current [*Sturges and Blaha*, 1976; *Blaha and Sturges*, 1981; *Sturges*, 1993]. Some of these processes may affect the dynamics on the shelf, such as the Loop Current eddies that decay next to the slope and affect the currents in the outer shelf, the jets associated with eddy pairs that develop cross-shelf transports, and the western boundary current that affects the coastal sea level and the outer shelf. In an excellent review of the dynamics of the shelves in the eastern Atlantic coast and the GoM, *Boicourt et al.* [1998] suggest that on the Mexican shelf there is a current that seasonally reverses. They made this conjecture on the basis of the analysis of AVHRR images and coastal zone color scanner images by *Biggs and Müller-Karger* [1994] that suggest that the fall-winter coastal current observed along the LATEX shelf continues at least as far south as Tampico, in southern Tamaulipas, and on data reports of currents 30 km offshore Tuxpan (21.6°N, 97.1°W) and Veracruz Port that show downcoast currents in fall and winter and upcoast currents in spring and summer [*Gutiérrez de Velasco et al.*, 1992, 1993]. The analysis of surface drifters deployed in 1998 shows a downcoast current along the Mexican shelf during the fall [*Lugo-Fernández et al.*, 2001]. Studies in the Bay of Campeche have shown that there is a mean cyclonic circulation [*Vázquez*, 1993] that has a seasonal cycle [*Monreal et al.*, 1992], but they did not study specifically the shelf dynamics. However, it has been reported that on the southern Tamaulipas-Veracruz (TAVE) shelf the water column is mixed in winter and stratified in summer [*Soto and Escobar*, 1995]. On the Campeche Bank, a westward current has been suggested [*Monreal et al.*, 1992; *Merino*, 1997].

[5] This paper describes the main characteristics of the seasonal circulation on the western shelf of the GoM and discusses the dynamics of the circulation features. This study is based on the results of a very high-resolution numerical simulation of the entire GoM, and on the analysis of hydrographic, sea level, AVHRR, and SeaWiFS data. In section 2 we briefly describe the numerical model and the analyzed data. Results are presented in section 3, and sections 4 and 5 include some discussion and conclusions.

2. Model and Data

[6] In this study, The Navy Coastal Ocean Model (NCOM) is used to simulate the GoM [*Martin*, 2000; *Morey et al.*, 2003a]. The NCOM is a primitive equation hydrostatic model with the Boussinesq approximation. It is similar in its physics and numerics to the Princeton Ocean Model (POM) [*Blumberg and Mellor*, 1987], but has some additional physical and numerical options. A remarkable difference from the POM is the use of hybrid coordinates that allows the use of sigma layers near the surface and geopotential (z) level vertical coordinates below a specified depth. These characteristics make the NCOM a good model for the study of coastal currents, regions with large salinity and temperature gradients, and the influence on the shelf of the rich eddy field of the offshore environment in the GoM. The model domain includes the whole GoM and the western Caribbean Sea, from 98.15°W to 80.60°W and from 15.55°N to 31.50°N, with model equations discretized on a 1/20° grid in latitude and longitude. There are 20 sigma layers uniformly distributed in the upper 100 meters, and 20 unevenly distributed z level layers below 100 m. The model is run using the Mellor-Yamada Level 2 turbulence closure scheme for vertical mixing, quasi-third-order upwind advection of scalars and momentum, and second-order calculations of the vertical advection terms, horizontal pressure gradient terms, and interpolation of the Coriolis term. Initial temperature and

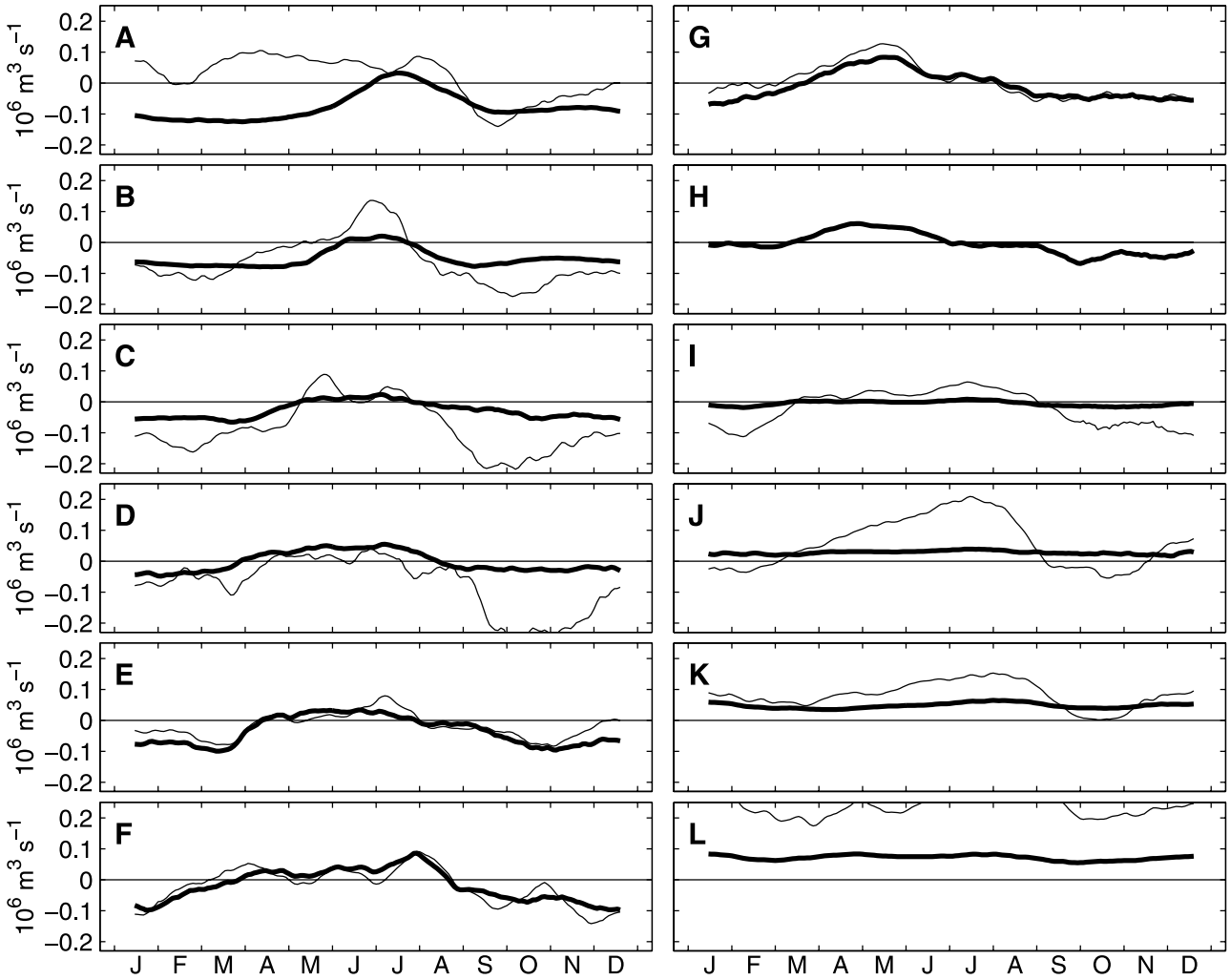

Figure 2. Transports, filtered with a 30-day running average, across the sections indicated in Figure 1. Thick lines indicate the transports between the coast and the 25 m isobath from surface to bottom. Thin lines indicate the transports between the 25 m and 50 m isobaths. Positive values indicate upcoast transports.

salinity fields are derived from the 1994 World Ocean Atlas [*National Oceanic and Atmospheric Administration*, 1994]. The model is forced with climatological monthly surface fluxes of heat and momentum derived from the Comprehensive Ocean Atmosphere Data Set [*DaSilva et al.*, 1994]. The discharge of 30 major rivers is prescribed using monthly means for those in the United States and annual means for those in Mexico. A surface salinity flux uniform in space and time is also applied to balance the riverine input of fresh water. Climatological volume flux at the open boundary in the Caribbean Sea is calculated from a mean dynamic topography relative to 1000 m, derived from historic hydrographic measurements [*Fox et al.*, 2001], and to a baroclinic velocity profile dynamically consistent with the climatological temperature and salinity fields.

[7] The simulation reproduces well the large-scale features in the GoM, such as the Loop Current and the associated large anticyclones. The mean northern penetration of the Loop Current in the model is approximately 26.5° N, compared to 27° N from the mean dynamic topography relative to 1000 m [*Fox et al.*, 2001], and to the average of 27.5° N calculated from five years of satellite data [*Vukovich*, 1988a, 1988b]. The mean transport between the Yucatan Pensinsula and Cuba is 32 Sv (1 Sv = 10^6 m s^{-1}), which is somewhat larger than previous estimates [*Gordon*, 1967; *Roemmich*, 1981] and the recently measured 23.8 Sv by *Sheinbaum et al.* [2002]. The simulation generates a similar current structure in the Yucatan Channel to that obtained from recent measurements [*Ochoa et al.*, 2001; *Sheinbaum et al.*, 2002], with the core of the current confined to the upper 800 m on the western side of the Channel, a countercurrent in the Cuban side, and two deep countercurrents along the eastern and western slopes [*Morey et al.*, 2003a]. The Loop Current sheds large anticyclones at irregular intervals, varying from 2.7 to 15 months, with a mean of 9.9 months, similar to the results reported by *Sturges and Leben* [2000] for a 30-year period. In the model the average westward trajectory of the Loop Current eddies reaches the western GoM around 26° N, which is slightly north compared to the observed trajectory that reaches the western GoM around 24.5° N. The model also simulates well smaller-scale features, such as the small

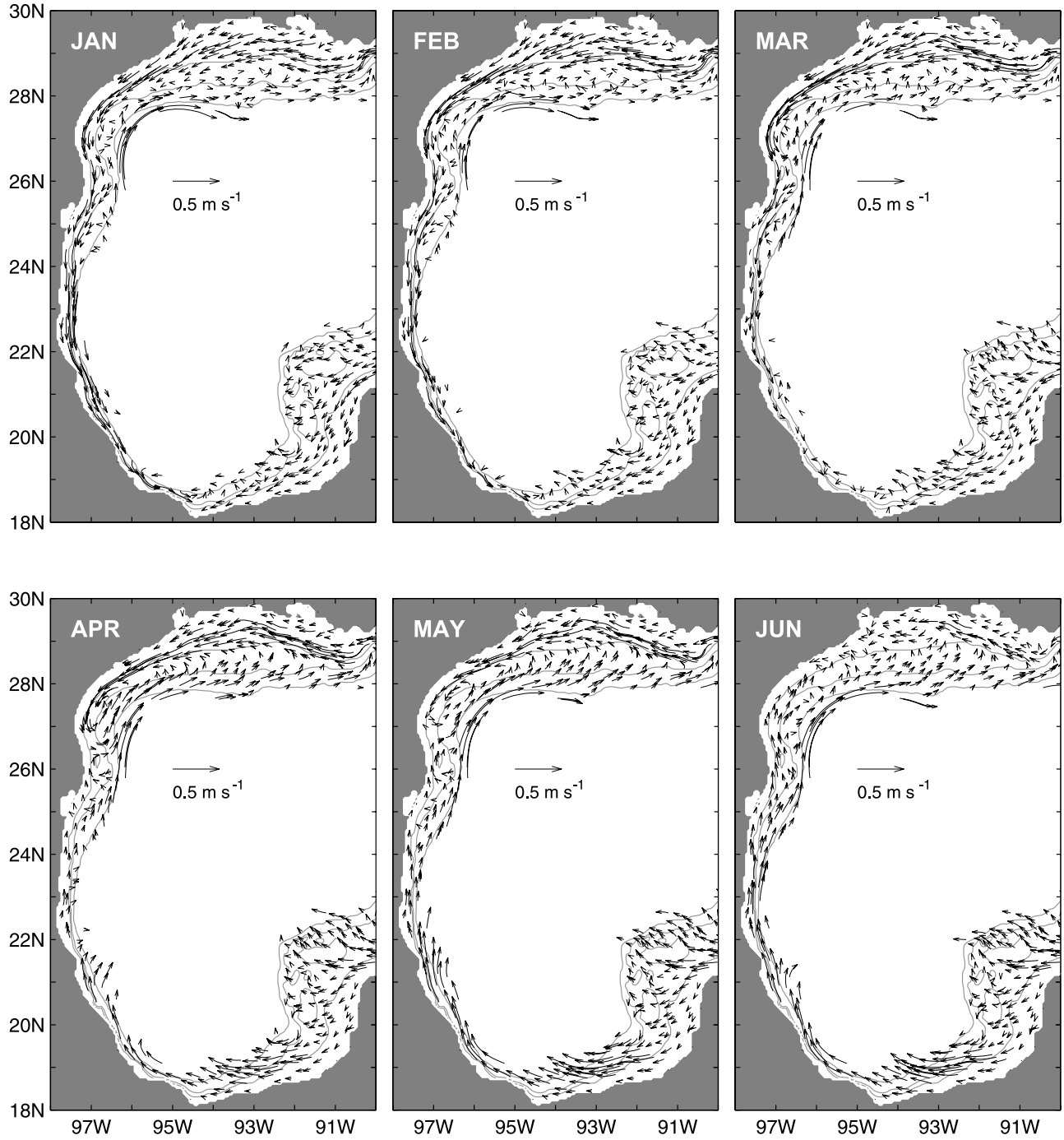

Figure 3. Monthly mean surface currents from 7 years of model data along the western shelf of the Gulf of Mexico. Shown are the isobaths of 25, 50, and 200 m.

frontal eddies along the Loop Current, the frontal instabilities along the western continental shelf, later discussed in this paper, and small eddies and filaments on the West Florida Shelf. In this study, the last seven years of a 10-year model simulation are analyzed. Detailed information of the NCOM and the GoM simulation are given by *Martin* [2000] and *Morey et al.* [2003a], respectively.

[8] Several sources of hydrographic data are used for this study: historical data from the National Climatic Data Center, data from several cruises in the Mexican shelf kindly provided by Luis Soto from the ICML-UNAM, and data from *Vidal et al.* [1988, 1990, 1994b]. The salinity data from some cruises required calibration. For those cruises in which there were deep casts, the salinity was adjusted to the climatology by linear regression. If there were no deep casts or the salinity data had many spikes, the data were discarded.

[9] In addition, monthly mean sea level data from tide gauges obtained from *González et al.* [1997], sea level atmospheric pressure data from the NCEP Reanalysis provided by the NOAA-CIRES Climate Diagnostics Center, Boulder, Colorado, USA (http://www.cdc.noaa.gov), and

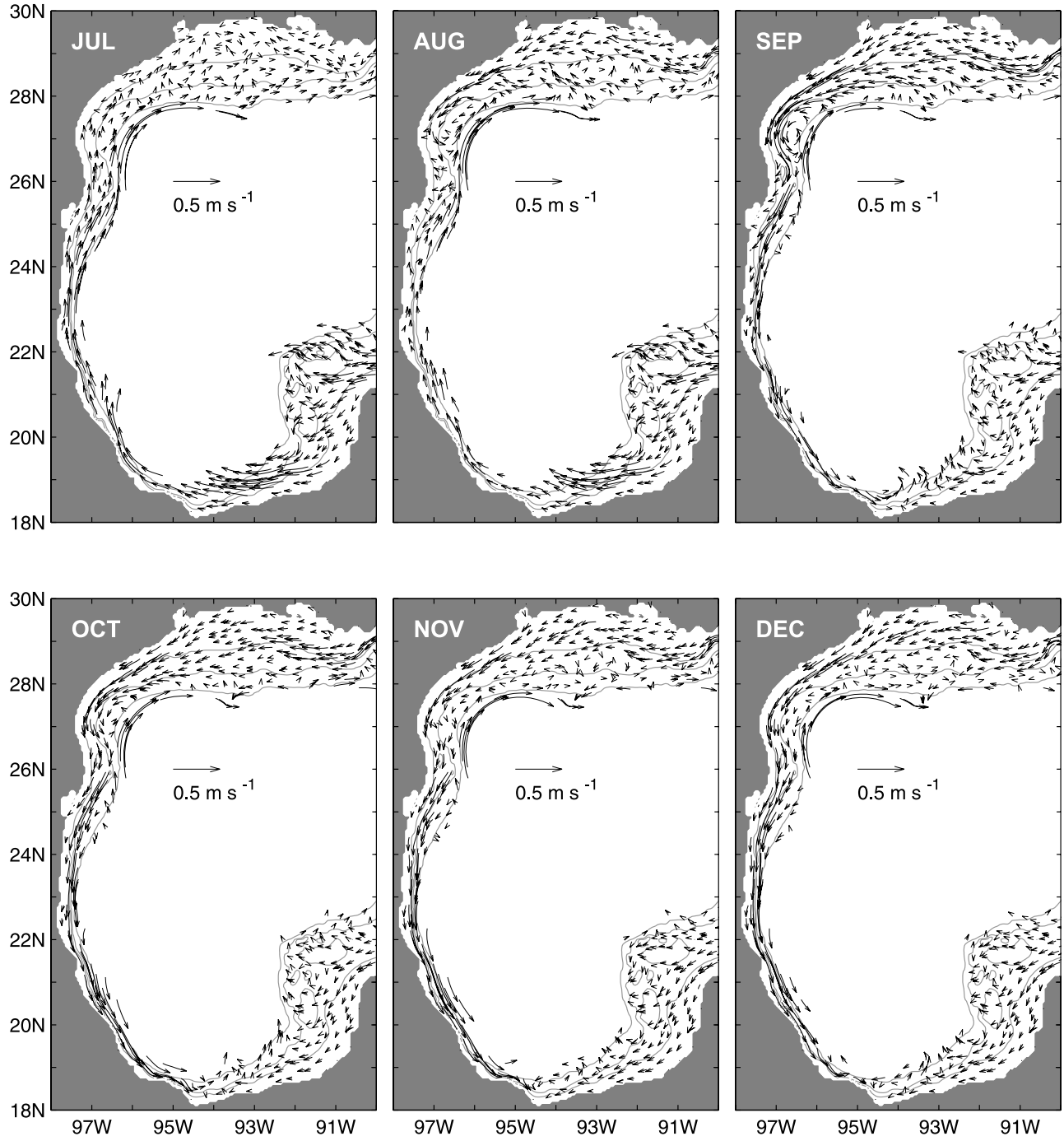

Figure 3. (continued)

monthly mean chlorophyll *a* concentrations estimated from the SeaWiFS data are considered. AVHRR images were processed at IG-UNAM.

3. Results

[10] On a seasonal scale the circulation over the LATEX shelf is well known, but there are considerably fewer studies south of the Rio Grande mouth. Here, the discussion frequently refers to the LATEX shelf in order to relate its dynamics to that of the Mexican shelf and as a reference to compare model results with previous works. Results are also compared with available data from the Mexican shelf.

3.1. Along-Shelf Transports and Surface Currents

[11] Transports on the western shelf of the GoM, calculated by horizontally and vertically integrating model velocities, have a strong seasonal component but with regional differences. In order to evaluate their behavior along the western shelf, transports are computed across several meridional or zonal sections (Figure 1). From the Rio Grande to the southernmost part of the Bay of Campeche the main transports are as follows: from September to

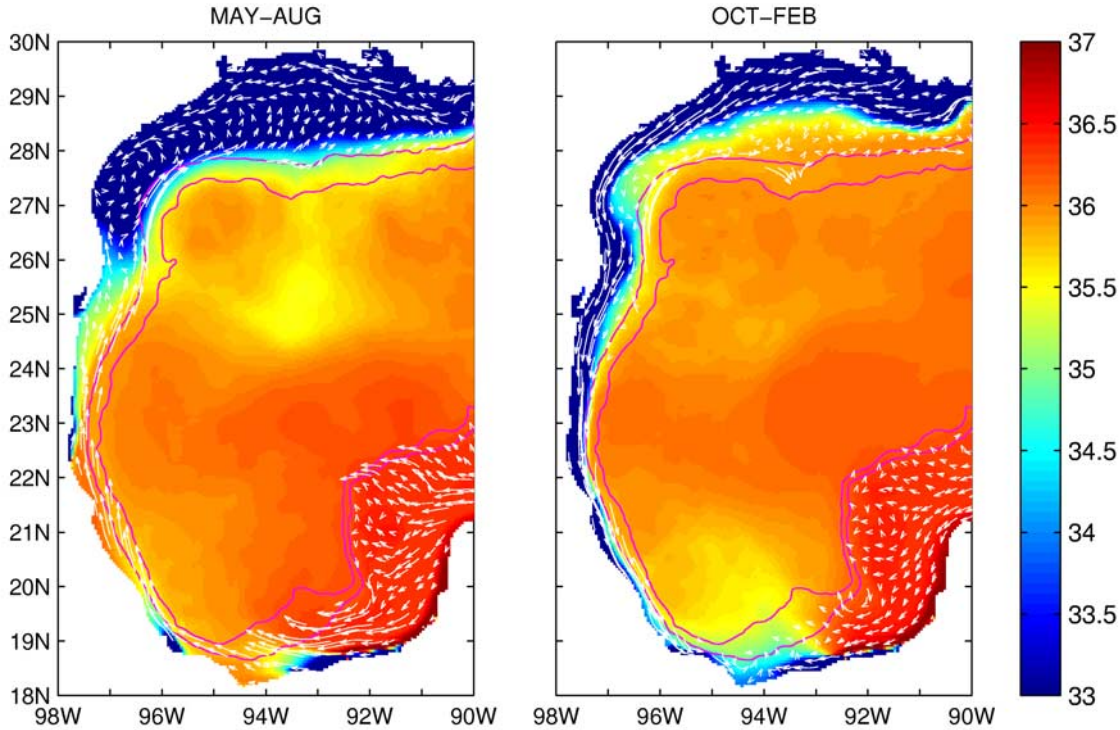

Figure 4. Mean surface salinity from the model output for: (a) May to August and (b) October to February. Vectors represent the main currents for the period with the same scale as in Figure 3. Shown are the 200 m and 1000 m isobaths.

March, the transports across sections between the coast and the 25 m isobath, and between the 25 m and 50 m isobaths, are downcoast (Figure 2). From May to August the circulation reverses and transports are upcoast over the TAVE shelf. The period of the upcoast circulation is shorter than that of the downcoast circulation and reduces progressively to the north and east along the LATEX shelf. At section C, the upcoast circulation period reduces to less than three months, from middle May to early August; on the LATEX shelf at section B, it decreases to less than two months, from early June to late July, and is nearly limited to July at section A. Along the western Campeche Bank the circulation is upcoast throughout the year; in the middle shelf the transport has a maximum in July that drops almost to zero in September and remains weak until March, increasing slowly until June. In the Bay of Campeche, between sections I and J, during the fall-winter period there is a confluence region produced by a downcoast coastal current on the TAVE shelf and an upcoast current on the western Campeche Bank. This confluence generates an offshore transport, which is discussed in detail later on. In the southern Texas shelf, between sections C and D, there is another confluence region with its corresponding offshore transport, although most of the time the offshore transport recirculates within the shelf. The confluence regions, the current reversal on the TAVE shelf, and the recirculation on the LATEX shelf are clearly identifiable in the 7-year monthly mean surface currents (Figure 3).

[12] Although the transports in the outer shelf are influenced by the eddies, one major characteristic of the LATEX shelf during the fall, winter, and spring seasons is that, while over the inner shelf there is a westward current, on the intermediate and outer shelf the mean current is eastward. This characteristic can be observed in the transports between the 25 m and 50 m isobaths at the meridional section A, and in the mean surface currents. The countercurrent is driven by the anticyclones that decay next to the slope as was reported by *Nowlin et al.* [1998]. The shear within the shelf is also observed in the mean surface currents at the southern part of the Texas shelf and the northern Tamaulipas shelf (Figure 3). It is noticeable that the transition from downcoast to upcoast in the north TAVE shelf frequently begins with the coexistence of downcoast currents in the inner shelf and upcoast currents in the outer shelf, few days later the downcoast current weakens and vanish. The inner shelf preference of the downcoast current is consistent with its lower density, because of the lower salinity.

[13] The current reversal does not occur simultaneously along the entire western shelf. It happens between August and September, beginning in the north and propagating downcoast with approximately a 1-month lag between the LATEX shelf and the southern Bay of Campeche. On the western Campeche Bank, the transports between the 25 m and 50 m isobaths have a strong seasonal signal with a peak in July–August and a minimum in November (Figure 2), although there is not a low-frequency current reversal over the inner shelf. During the spring transition, from March to April, the reversal in the current direction begins in the south and moves northward, also with about a 1-month lag from section I and section E (Figure 3).

3.2. Confluence Regions

[14] The downcoast circulation on the TAVE shelf during the fall-winter season reaches the southernmost part of the

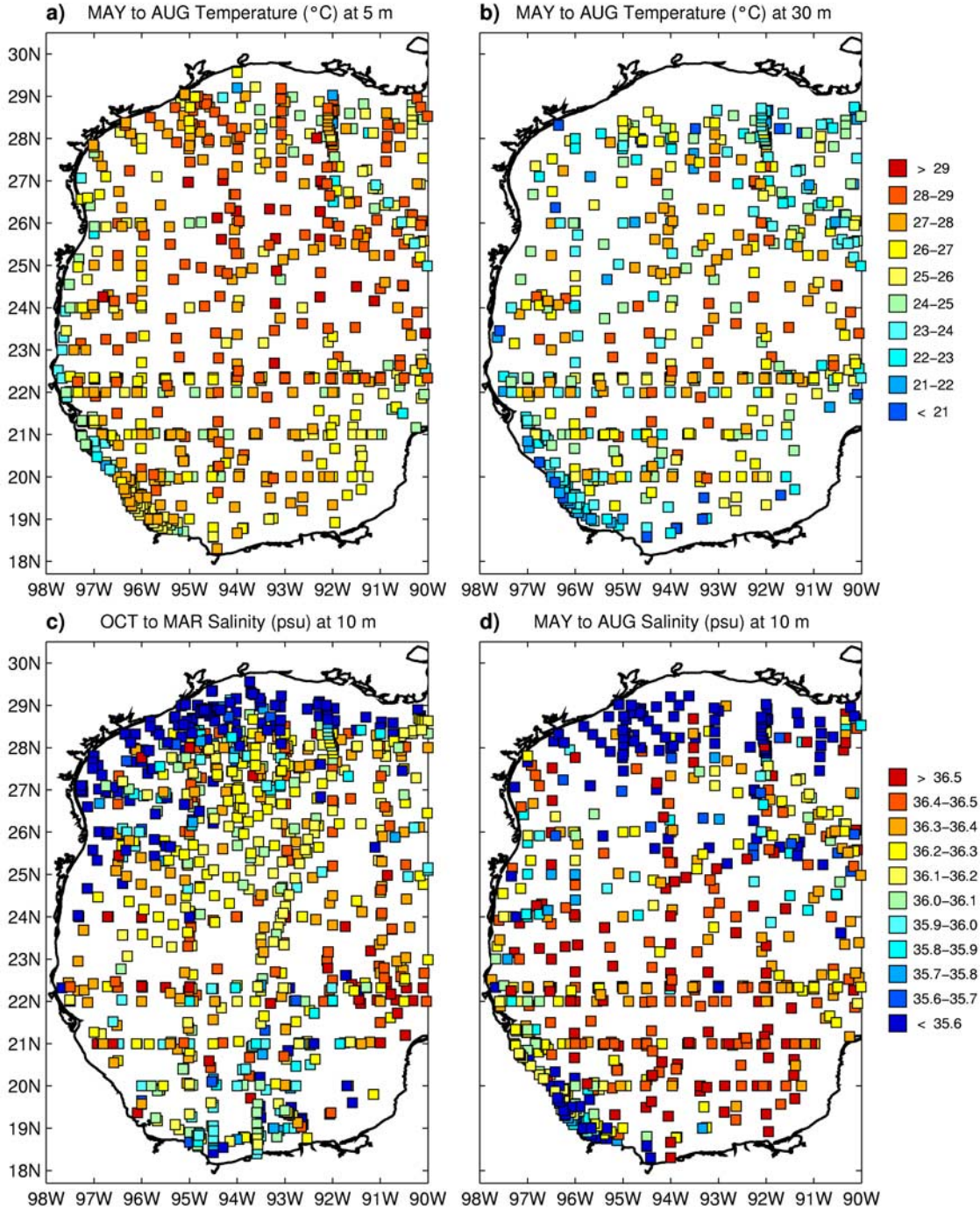

Figure 5. Individual temperature and salinity observations from historical hydrographic data. Temperature from May to August (a) at 5 m depth and (b) at 30 m depth. Salinity at 10 m depth (c) from October to March and (d) from May to August.

Bay of Campeche, between sections I and J, where it meets an opposing current. This confluence generates an offshore transport of at least 0.1 Sv. An indication of the offshore transport is the seasonality of the low-salinity water in the southern part of the Bay of Campeche in both model and historical hydrographic data (Figures 4 and 5). This water comes from remote and local rivers, mainly the Coatzacoalcos and Grijalva-Usumacinta. Off-shelf transports are also noticeable from hydrographic data with lower-salinity values in the fall-winter than in the summer, when the river discharges peak. The impact of off-shelf transports may be of particular significance because the southern Bay of Campeche is an important fishery and oil extraction region [*Soto and Escobar*, 1995].

[15] The other confluence region is on the southern Texas shelf, between sections C and D. This confluence is stronger in April and May. Offshore transports in this region have been reported previously [*Müller-Karger et al.*, 1991; *Biggs and Müller-Karger*, 1994; *Walker et al.*, 1996], being identified because of the relatively high chlorophyll *a*

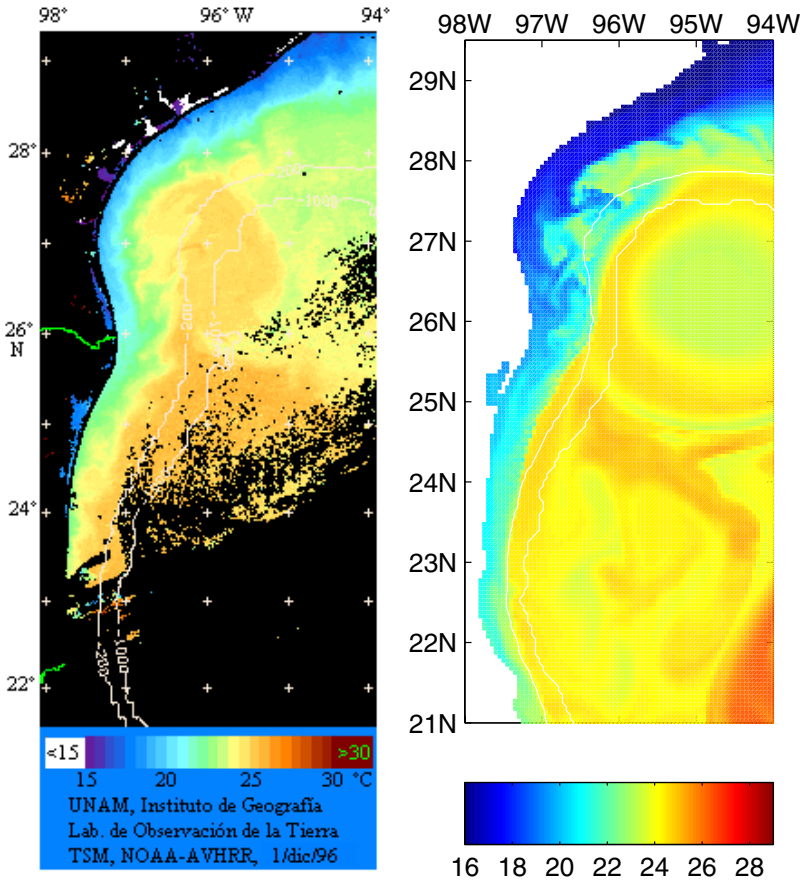

Figure 6. (left) Sea surface temperature from NOAA-AVHRR satellite data during 1 December 1996 and (right) model sea surface temperature for a particular day in December. Note the presence of cold water along the western shelf. The 200 m and 1000 m isobaths are shown.

content of the inner shelf waters. The offshore transports sometimes cross the shelf break because of the jets associated with the edge of an eddy or a pair of eddies. Most of the previously reported off-shelf transports were of this category but, from the 7-year mean model simulation, it is found that the offshore transports have a seasonal preference that may modulate the cross-shelf transports favored by the presence of eddies.

[16] The convergence of along-shelf currents on the western shelf is compensated by offshore transports mainly located in the southern Bay of Campeche, where opposing currents meet in fall and winter, and in the southwest of the LATEX shelf. The offshore transports are balanced by the input of water from the eastern Bank of Campeche, east of 90°W, and by fluxes onto the eastern LATEX shelf from offshore and the east.

3.3. Temperature and Salinity Fronts

[17] During the fall and winter, low-salinity water from the Mississippi-Atchafalaya river system is advected onto the TAVE shelf, along the inner LATEX shelf, developing sharp fronts on the Tamaulipas shelf close to the 50 m isobath. The fronts are detected in sea surface temperature satellite images and are found in the model results even though the model is forced with monthly mean fluxes (Figure 6). The advected water can be around 5 °C cooler than the water off the shelf.

[18] During summer, when the circulation on the Tamaulipas shelf reverses, the Mississippi-Atchafalaya water does not reach the Tamaulipas shelf and remains recirculating within the LATEX shelf, or is advected eastward of the Mississippi River mouth (see Figure 4). This result is consistent with previous studies on the seasonal circulation of the LATEX shelf [*Cochrane and Kelly*, 1986; *Li et al.*, 1996; *Cho et al.*, 1998; *Nowlin et al.*, 1998] and studies on the fate of the river discharged water in the northern gulf [*Morey et al.*, 2003a, 2003b]. The main contribution of fresh water to the TAVE shelf comes from the local rivers, mostly from the Grijalva-Usumacinta, Coatzacoalcos, Papaloapan, and Pánuco. These rivers are relatively small compared to the Mississippi and Atchafalaya, so, although they discharge directly onto the TAVE and Tabasco shelves and have a maximum discharge in summer, the amount of fresh water on the northern TAVE shelf is larger in winter. The Rio Grande discharge is insignificant because of the Falcon and La Amistad dams that store most of the drainage of the Rio Grande basin.

3.4. Vertical Structure

[19] The vertical structure of the water column on the western shelf of the GoM also has a strong seasonality. In fall-winter, the TAVE shelf is characterized by the frequent occurrence of temperature inversions, which are statically stable because of the surface low-salinity water. The inver-

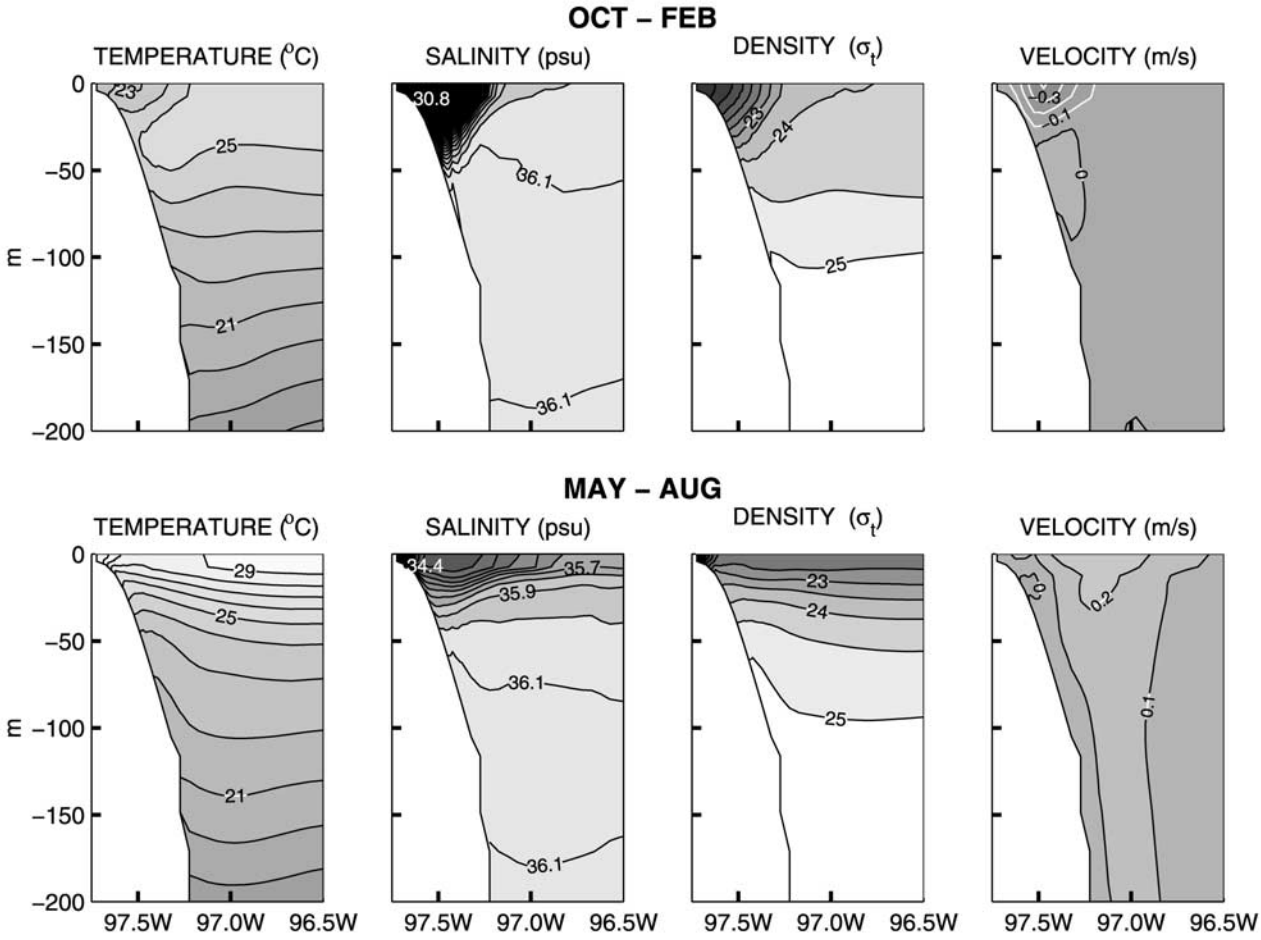

Figure 7. Monthly mean vertical structure from model output in section E of Figure 1, averaged from (top) October to February and (bottom) May to August of 1 year.

sions of temperature, which are evident even in the seasonal mean, are caused by the advection of cold low-salinity water from the LATEX shelf (Figure 7). Model results are supported by hydrographic data from different cruises and profiling floats that show the low surface salinity and the vertical temperature inversions [*Vidal et al.*, 1988; *Weatherly et al.*, 2003].

[20] During the summer, the vertical stratification increases since the upper ocean becomes warmer and there is more offshore penetration of the upper layer low-salinity water, distinctively in the region with stronger river influence. Model results suggest that from April to August there is upwelling on the TAVE shelf, with a peak in July, as seen by the on-shelf penetration of intermediate depth water from off of the shelf (Figure 7). The relatively cold water barely reaches the surface, probably because of the strong stability of the warm fresh upper layer. This result is consistent with the upwelling for the southern LATEX shelf reported by *Nowlin et al.* [1998] and with hydrographic data from several cruises as can be observed in temperature maps from historical data (Figures 5a and 5b).

3.5. Sea Level

[21] The sea level is the only variable that has been measured systematically in the western GoM. Four tide gauge stations representative of the western shelf of the GoM are analyzed: Galveston, Cd. Madero, Veracruz, and Progreso (Figure 8a). A characteristic of the annual variability of the sea level is its similarity within a region of more than one thousand kilometers along the coast. All the stations have a maximum sea level in September–October. It peaks in Galveston during September and leads the other three locations by one month. This maximum is also observed in the model sea surface height (SSH) results and in tide gauge observations, but the model has 1-month lag in Progreso (Figure 8b).

[22] Tide gauge data show a second sea level maximum during May, which is more intense in Galveston than in the other three locations. This secondary maximum is well reproduced by the model for Galveston but not for the other locations, showing smaller amplitudes. Between the maxima there are two minima, one in July and the other in January–February that have smaller amplitude and are less consistent among the stations than the September–October maximum (Figure 8b). The Progreso sea level climatology has a slightly different pattern than the data from the other three tide gauge stations; it has the October maximum and the relative maximum in May, but the minima are reached in March–April and June. The model sea level signal reproduces between 30% and 76% of the observed variance (Figure 9).

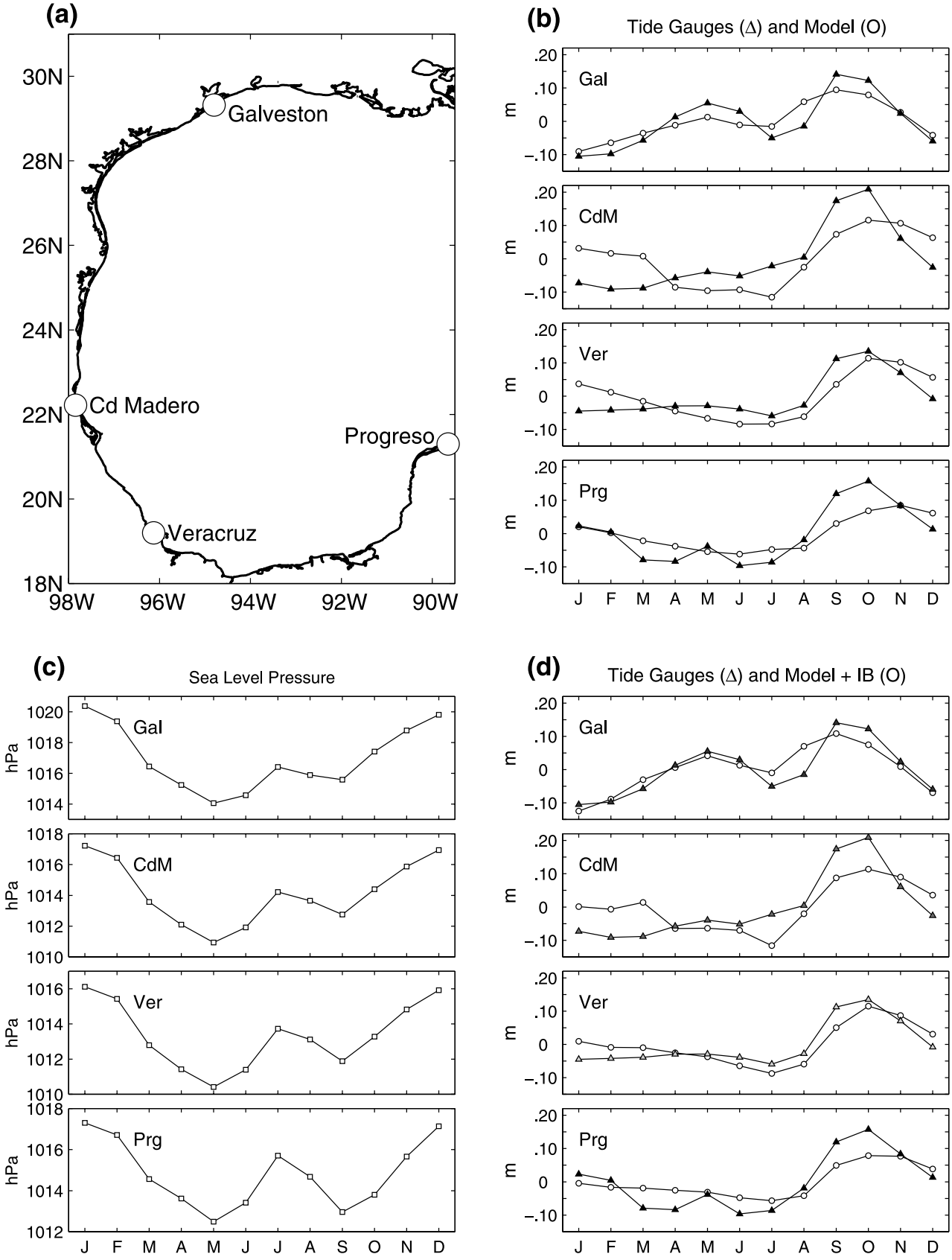

Figure 8. (a) Location of four tide gauge stations, (b) monthly mean sea surface height from tide gauge stations (triangles) and from the model (circles), (c) monthly mean sea level atmospheric pressure, and (d) monthly mean sea surface height from tide gauges (triangles) and from model with the inverse barometer effect (circles). Standard deviations of model data are less than 1 cm.

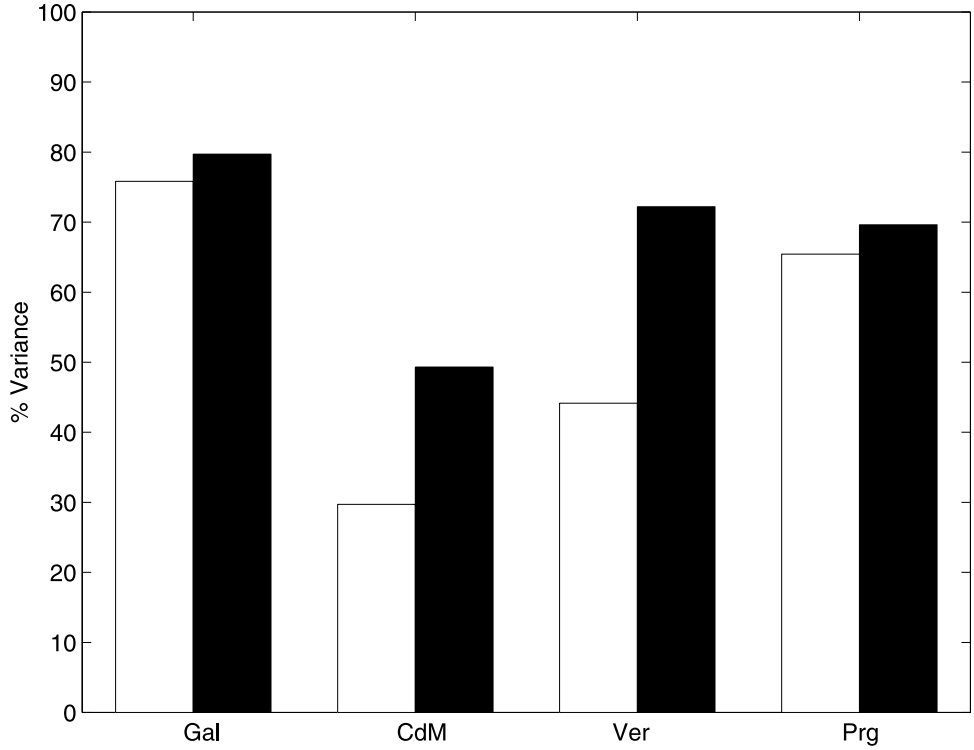

Figure 9. Percentage of the monthly mean sea level variance explained by the model (white bars) and by the model with the inverse barometer contribution (black bars) for Galveston (Gal), Cd. Madero (CdM), Veracruz (Ver), and Progreso (Prg).

[23] The simulated SSH from the model does not include the inverse barometer contribution due to changes of the atmospheric sea level pressure at the seasonal frequency. The sea level pressure has a clear seasonal pattern in the region, with an absolute maximum in December–January, a secondary maximum in July, and minimum values in May and September. On the basis of the NCEP-Reanalysis product, the pressure difference between the highest (January) and lowest (May) values is around 6 hPa for the four locations, and between the secondary maximum in July and the absolute minimum in May is around 4 hPa. The pressure difference between July and September is smaller in Galveston, Cd. Madero, and Veracruz than in Progreso by around 2 hPa (Figure 8c). The low-frequency variability of the sea level atmospheric pressure does not have a direct impact on the dynamics of the ocean but affects the sea level at a rate close to -1 cm per each hPa. The addition of the inverse barometer contribution to the model sea level yields a better agreement with the observed sea level (Figure 8d) and increases the percentage of the sea level variance explained by the model output to a range between 70% and 80% for Galveston, Veracruz and Progreso, and to 50% for Cd. Madero (Figure 9). The sea level from the model with the inverse barometer contribution reproduces well the September–October maximum and the July minimum but with smaller amplitude in both cases (Figure 8d). Model results lead the observed July minimum in Veracruz and Cd. Madero by one month. The model does not agree well with observations for the first four months of the year, when the observed sea level signal is weak, except at Galveston. Other contributions to the low-frequency sea level variability are not considered, such as the steric anomaly, which is a basin-scale contribution with amplitude of around 2 cm [*Greatbatch*, 1994; *Mellor and Ezer*, 1995], and the astronomical annual tide component, that has a similar contribution.

4. Discussion

[24] *Cochrane and Kelly* [1986], *Cho et al.* [1998], and *Nowlin et al.* [1998] showed that, for most of the LATEX shelf, there is a high correlation between the along-coast wind stress component (ACWSC) and the local currents. They identified a region of convergence of the ACWSC along the southern coast of Texas and a divergence near 93°W. *Cho et al.* [1998] confirmed that the main circulation over the LATEX shelf is wind driven.

[25] The ACWSC is the dominant forcing of the coastal circulation when it has a relatively small spatial and temporal variation; that is, the timescale of interest is greater than the inertial period and the scales of the along shelf currents and the wind field are larger than the width of the shelf. Over the western shelf of the gulf, the scale of the along shelf currents is relatively large compared to the width of the shelf, around 500 to 800 km compared to 50 to 100 km respectively; that is, the distance where the along-shelf currents are highly correlated. It is also required that the Rossby number (R = V/f L) be small; that is, the nonlinear terms are relatively small compared to the Coriolis force terms. Over the western shelf of the GoM currents are ~ 0.5 m s^{-1} so, considering L $\sim$ 100 km and $F = 6 \times 10^{-5}$ s^{-1}, R $\approx$ 0.08, but in the confluence regions L is

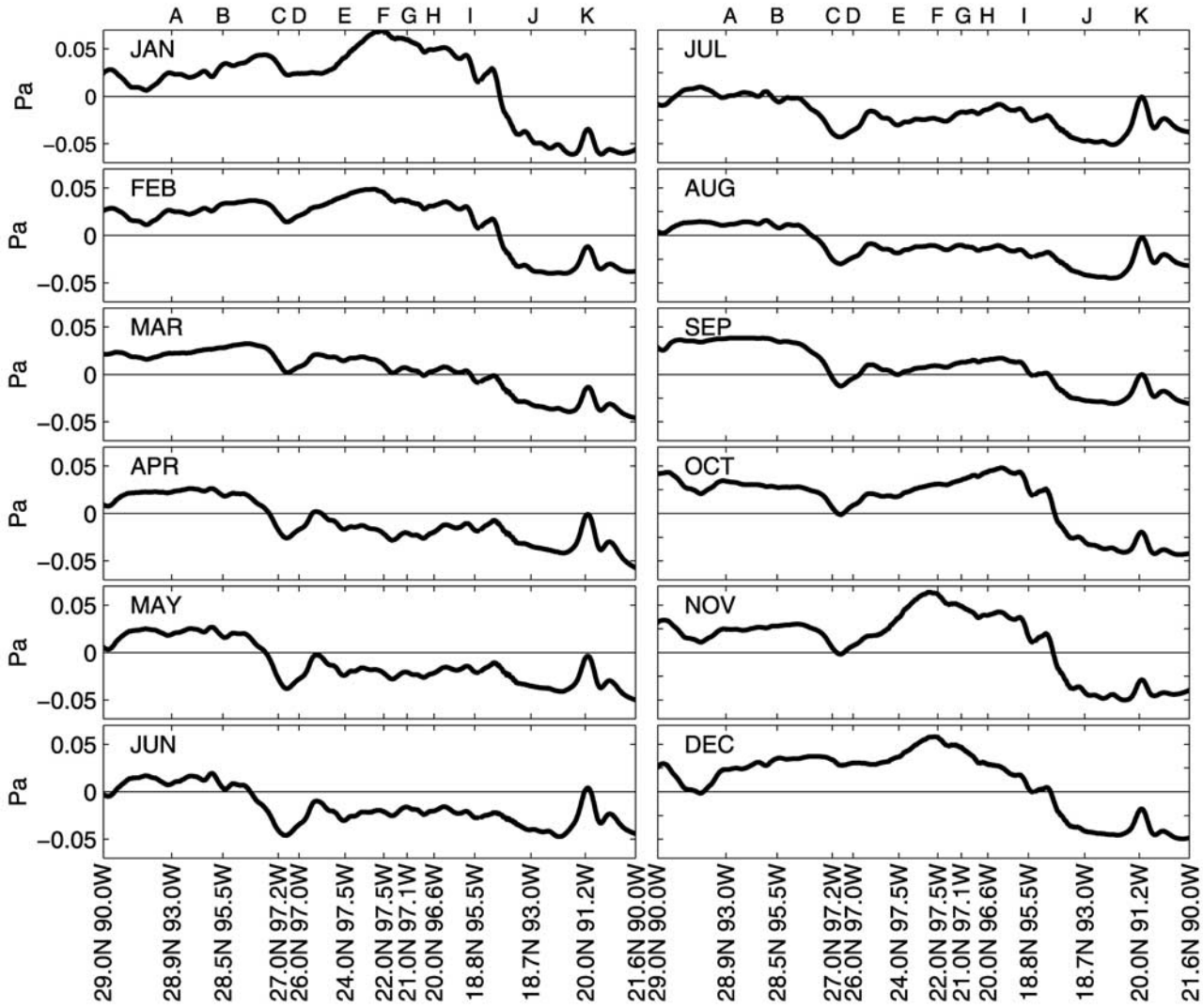

Figure 10. Monthly means of the along-coast wind stress component computed over a smoothed 25 m isobath. Positive values indicate downcoast direction.

smaller and R could be large enough to make the nonlinear terms important.

[26] The ACWSC is the principal forcing mechanism of the western shelf of the GoM, it explains the main features observed in the circulation. Along the Mexican states of Tamaulipas and Veracruz, between 18.5°N and 26°N, the ACWSC is upcoast from April to August and downcoast from September to March (Figure 10). In the Bay of Campeche, east of 95.5°W, the ACWSC has an upcoast direction during the whole year and is more intense in winter. The ACWSC has a small-scale variation associated with the coastline variations along the western Campeche Bank. In the LATEX shelf the upcoast ACWSC reaches the western shelf in July and is very weak in the eastern and central shelf. The reversal period in the *DaSilva et al.* [1994] climatology is limited to July, which is different from the observations for the summers of 1992 to 1994 when the upcoast ACWSC last for two months and was stronger [*Nowlin et al.*, 1998].

[27] The direction of the winds in the GoM is determined by the seasonal position of the high-pressure systems: in the fall and winter high-pressure systems move from the northwest continental United States into the gulf generating northeasterly winds in the western gulf, while in the summer the intensification and westward displacement of the Bermuda High and the warming of the continental United States generate southeasterly winds. The meridional component is intensified in the western gulf by the blocking effect of the Sierra Madre Oriental mountain range that has an elevation of around 2000 m. The development along the year of these high-pressure systems results in a bimodal evolution of the sea level pressure over the GoM, with maxima in winter and July (Figure 8c).

[28] The strongest and most variable coastal currents, at the seasonal frequency, of the western shelf are on the TAVE shelf, reaching a magnitude of more than 0.70 m s^{-1}. At the seasonal frequency, the winds in this region are also more intense and variable than over the rest of the western shelf. The correlation between the ACWSC and the 7-year model monthly mean along shelf currents is larger than 0.90, suggesting that this is the main forcing mechanism of the low-frequency shelf currents in this region (Figure 11).

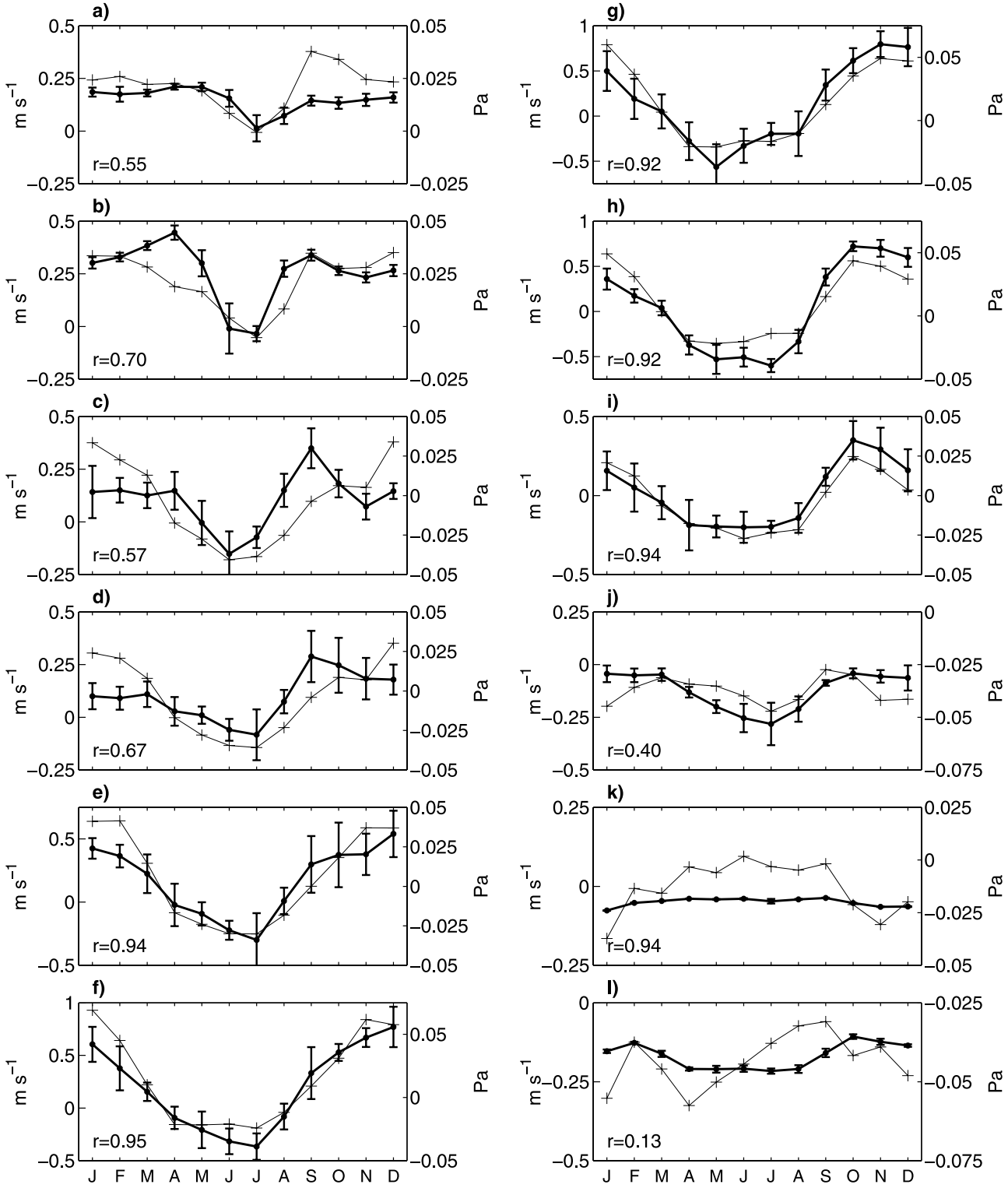

Figure 11. Monthly mean surface currents from 7 years of model data at locations indicated in Figure 1 (circles) and monthly mean of the along-coast wind stress component at the corresponding section (pluses). The values of the correlation coefficients are also indicated in each plot. Error bars represent one standard deviation. Positive values indicate downcoast currents and wind stress.

In the southern part of the Bay of Campeche, at 93.0°W, the correlation decreases significantly because of the high variability in space of the ACWSC (see Figure 10). In that region, offshore transports are important during fall and winter because of the confluence of currents, the along shelf currents vary over relatively short scales, therefore the Rossby number may not be small and the nonlinear terms significant. The variability of the monthly mean currents on

the western Campeche Bank (Figure 3), measured as the difference between the maximum and minimum values, is less than 0.10 m s^{-1}, while in the TAVE shelf it is greater than 1.00 m s^{-1}. The variability of the wind forcing is also smaller over the western Campeche Bank than in other areas of the western GoM. Therefore the correlation coefficient between the ACWSC and the surface currents is meaningless. The monthly mean transports and surface currents on the western Campeche Bank suggest that the main forcing is the local ACWSC, which is very stable throughout the year, and that the relatively small variability is produced by remote forcing due to long wavelength coastal waves associated with the changes in the circulation on the TAVE and LATEX shelves.

[29] The standard deviations of the monthly mean surface currents is very informative about how the wind forcing and the eddies affect each region. The location of the core of the coastal current for each section is subjectively chosen and referred from here on as stations with the corresponding letter (Figures 1 and 3). The stations are located near the coast, between 15 and 30 km, but at different depths. When the shelf is wide the stations are in shallow water, near the 20 m isobath, as on the LATEX shelf and the Campeche Bank. When the shelf is narrow, the core of the current and the corresponding station, although closer to the coast line, are in deeper water, as is the case on the TAVE shelf.

[30] Since the model is forced with climatological winds, all the interannual variability in the along shelf currents is expected to be associated with the mesoscale eddies that interact with the slope. The eddies do not have a seasonal behavior, although they have preferred paths. Therefore, as expected, the sections located where the shelf is wide have smaller variance because of the small or negligible influence of the eddies over the inner shelf. At stations K and I at the Campeche Bank the variance is very small, also in the LATEX shelf in stations A and B. It is noticeable that during late spring and summer the variance is larger. This suggests that the eddies have more influence in this region when the ACWSC is very weak. On the TAVE shelf at stations D to H the variance is larger because the shelf is narrower but the signal and the correlations of the currents with the ACWSC are larger. The value of the correlation coefficient is statistically significant for the 95% confidence level for 12 points (10 degrees of freedom), when the correlations are larger than 0.58 and is significant for the 99% level for correlations larger than0.71. Stations E to I in the TAVE shelf have correlation coefficients larger than 0.90 supporting that the ACWSC is the main forcing.

[31] These results are consistent with the near surface drifters for summer and winter from 1989 to 1999 that show downcoast currents in winter and upcoast currents in summer [*Nowlin et al.*, 2001, Figures 5.2–4 and 5.2–5]. The University of Colorado GoM model results are also consistent with these results; the standard deviation on the TAVE shelf for their model is very large and mainly along coast, suggesting strong along shelf currents with large variability, which agrees with our results [*Nowlin et al.*, 2001, Figures. 5.3–1 and 5.3–2]. The results of this study for the LATEX shelf region agree with the seasonal circulation reported in previous studies [*Cochrane and Kelly*, 1986; *Cho et al.*, 1998, *Nowlin et al.*, 1998] that found that the main forcing in the LATEX shelf is the local wind stress. The correlation coefficients between the surface currents and the ACWSC are 0.70 and 0.55 at stations B and A, respectively. There is a cyclonic circulation with a downcoast coastal current during the nonsummer months and an upcoast current in July. The period of the upcoast circulation shortens toward the east (Figures 3 and 10). A careful analysis show that the summer ACWSC from the *DaSilva et al.* [1994] climatological wind is weaker and shorter than those observed between 1992 and 1994 by *Nowlin et al.* [1998]. This causes the period of upcoast current in the LATEX shelf in model results to be restricted to around 15 days per year, during July, compared with observations that reported a reversal of 2 months [*Nowlin et al.*, 1998]. The relatively small difference in wind direction is critical in the development of the upcoast current, being shorter and weaker in the simulation (Figure 3) than in observations.

[32] From the analysis of the ACWSC a main result is that the western shelf, as a whole, is a convergence region. This is because for most of the year the ACWSC has larger values in the north than in the south, with the gradients being more intense during fall and winter (Figure 10). A consequence is that there is a net export of water from the western shelf into the deep ocean. The mass is balanced by the influx from the eastern Bank of Campeche, entraining water from the Yucatan Current, and from the eastern LATEX shelf. The rivers' discharge has a small contribution to the volume balance. The transports in the inner and intermediate shelf are around 0.1 to 0.2 Sv, the Mississippi and Atchafalaya Rivers have an average discharge of 0.020 Sv with a peak in April of 0.035 Sv and a minimum in September. Other rivers have a smaller contribution. A region with strong convergence is the southern Texas shelf, between sections C and D, particularly from April to August. *Cochrane and Kelly* [1986] identified this convergence region, and a later study based on an optimally interpolated wind field derived from buoy data made a detailed description of the ACWSC and the convergence [*Nowlin et al.*, 1998], and our results corroborate this showing the link with the TAVE shelf winds. In this region, events of offshore currents can be identified through remote sensing since the entrained coastal water is cold with high chlorophyll concentration. Previous studies have shown cross-shelf transports in this region associated with the interaction of eddies with the slope [*Biggs and Müller-Karger*, 1994; *Müller-Karger et al.*, 1991], but these results show that the chlorophyll *a* content of the cross-shelf filaments may be modulated by the seasonality of the convergence of the ACWSC, being larger from April to August. The seasonality of the monthly mean upper ocean chlorophyll *a* content for the period 1997 to 2001 from the SeaWiFS is consistent with these results (Figure 12). The location of the eddies may determine if the offshore current crosses the shelf break or turns cyclonically onto the outer shelf. A second region of strong convergence is in the southernmost part of the Bay of Campeche, between sections I and J, most evident from September to February. In this region, model results show strong cross-shelf transports, which are evident because of the lower salinity of the shelf water. A maximum in the chlorophyll *a* content detected through SeaWiFS data during the fall and winter supports model results that suggest that the offshore transport is more intense during this period (Figure 12). The high

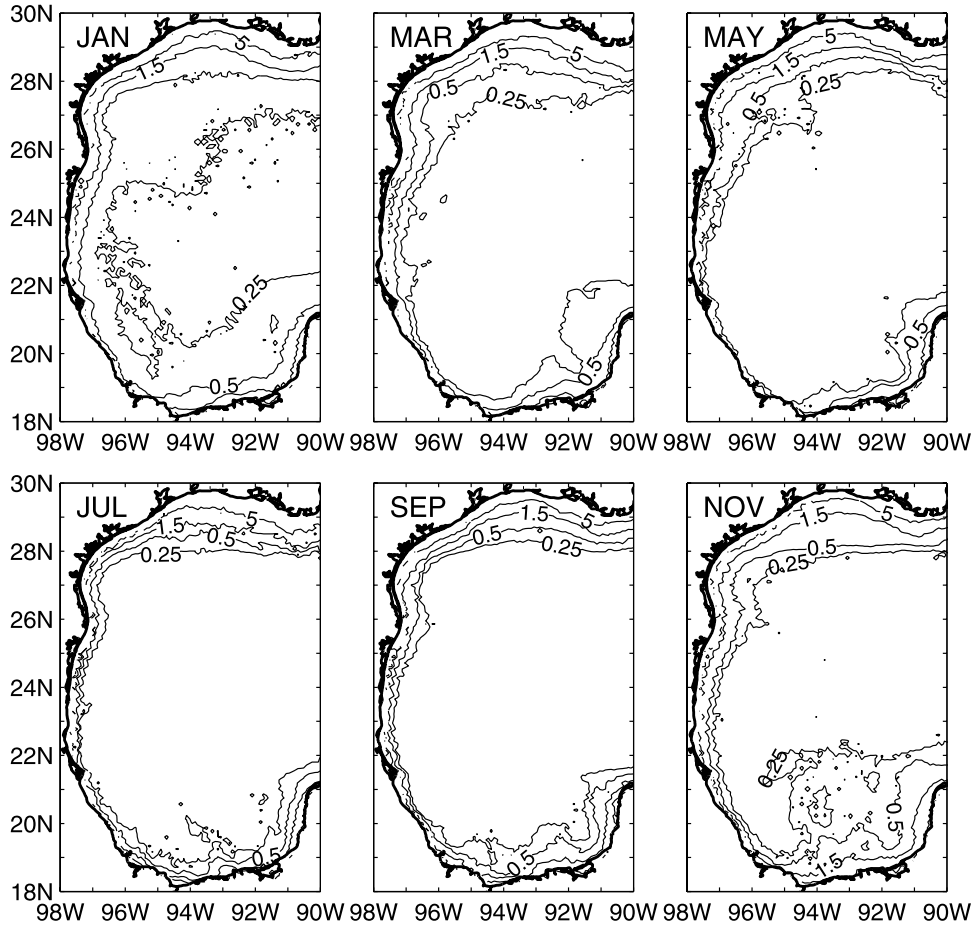

Figure 12. Monthly mean chlorophyll *a* content (mg m^{-3}) estimated from SeaWiFS data. Monthly means for January–April from 1997 to 2001, May–October from 1998 to 2002, and November–December from 1998 to 2001.

content of chlorophyll *a* during fall and winter in the Bay of Campeche does not seem to be produced by coastal upwelling due to Ekman transport since the northerly winter winds are downwelling favorable for the western side of the Bay and neutral for the southern. Although the winds are upwelling favorable for the eastern side of the Bay of Campeche, they are not significantly more favorable than in the summer. However, there may be a small contribution to the increase of nutrients in fall-winter because of the increase of entrainment into the mixed layer associated to the seasonal variation of the mixed layer depth, but this term is similar in other regions of the GoM.

[33] The distribution of low-salinity water and the sea surface temperature are also affected by the seasonal circulation. In the nonsummer months the low-salinity water from the Mississippi-Atchafalaya Rivers is advected along the LATEX shelf reaching the TAVE shelf and the southern Bay of Campeche, whereas from April to September the Mississippi-Atchafalaya Rivers low-salinity water does not reach the TAVE shelf. The weaker and shorter upcoast current along the LATEX shelf allows a more westward penetration of the low-salinity water in model results compared to observations (Figure 13). The fall sea surface salinity distribution is very similar to observations but with the low-salinity water slightly more coastally attached, which is expected because the variability of the synoptic-scale winds, which increases the mixing of the low-salinity water [*Garvin*, 2001], is not included in the forcing field. The water temperature over the shelf is also strongly determined by the circulation through the advection of low-temperature water from the LATEX shelf into the TAVE shelf. Model temperatures have a good agreement with observations (Figures 6 and 13). For the LATEX shelf, the agreement for the November sea surface temperature is within one standard deviation from the observations reported by *Nowlin et al.* [1998, Figure 4.2–16].

[34] The ACWSC also contributes to the seasonal variability of the vertical structure over the TAVE shelf. From April to August, the offshore surface Ekman transports of low-salinity water, the upwelling of deep water onto the shelf (Figure 7), and the positive heat flux into the ocean [*Zavala-Hidalgo et al.*, 2002], increase the stratification over the shelf, which has been reported previously [*Soto and Escobar*, 1995] and is supported by the relatively low subsurface temperature observed in the historical hydrographic data (Figure 5). The offshore Ekman component can be distinguished in the mean surface currents (Figure 3). From September to March, the downcoast ACWSC favors the piling of low-density water toward the coast and the coastal current is confined to the inner and intermediate

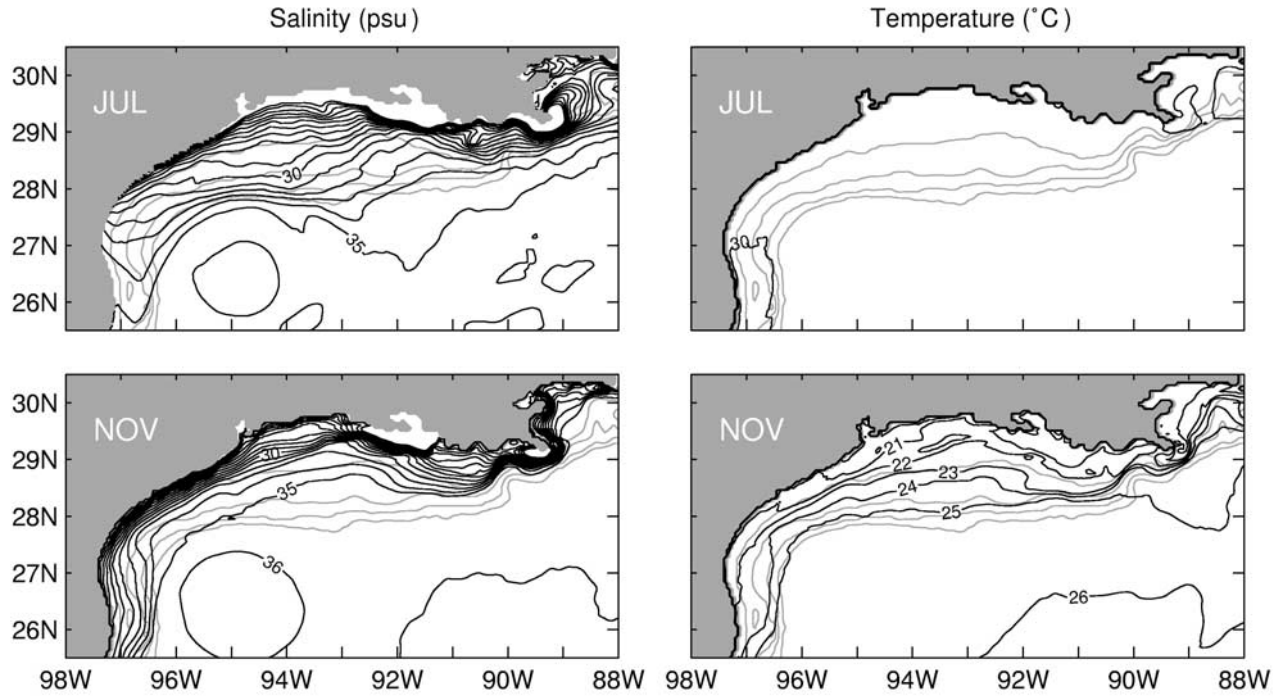

Figure 13. Model monthly mean sea surface salinity and temperature for July and November on the Louisiana-Texas shelf. Bathymetry contour lines of 25, 50, 100, and 200 m are shown.

shelf. The inshore Ekman transport together with the negative surface heat flux and the increase of turbulent kinetic energy in the upper ocean by the increase of the wind stress magnitude [*Zavala-Hidalgo et al.*, 2002], mix the water column and generate a horizontal gradient with low-density water near the coast (Figure 7).

[35] The seasonal variability of the sea surface height is mainly confined to the shelf, as can be seen in the cross-shelf gradients of SSH along the western GoM (Figure 14). Its seasonal range, measured as the maximum minus the minimum values, is larger at the coast than at the outer shelf, the shelf break, or the slope. At 26°N, the seasonal range is ~22 cm at the coast and ~10 cm at the shelf break; at 24°N the range is ~24 cm at the coast and ~12 cm 50 km off the coast, and at 20°N is ~18 cm at the coast and ~6 cm 40 km off the coast (Figure 14). These results show that the coastal currents within the shelf and the atmospheric sea level pressure are the major contributors to the seasonal sea level signal rather than a western boundary current as was proposed by *Sturges and Blaha* [1976], *Blaha and Sturges* [1981], and *Sturges* [1993]. However, although weaker, there is a seasonal signal at the slope that may be generated by a western boundary current as Sturges and Blaha suggested, but the causes of the SSH variability at the slope are not analyzed here. The peak of SSH is associated with the transition between upcoast to downcoast current and the displacement of the regions of stronger convergence. Since the SSH in Galveston leads by one month the peak on the locations downcoast, in model and tide gauges, it seems that the transition is not simultaneous but since the model is forced with monthly winds that cannot be definitively concluded. *Nowlin et al.* [1998] reported that the downcoast to upcoast transition in the LATEX shelf occurs in a period of several weeks and not simultaneously along the shelf but they found that the upcoast to downcoast transition occurs almost simultaneously.

[36] The SSH maximum in September–November and the minimum in July have a clear signal in all sections. The cross-shelf gradients of SSH at 26°N, 24°N, and 20°N, on the TAVE shelf, reverse along the year, as the along shelf currents do. In these sections the gradients point inshore from September to April and offshore from April to July. Over the western Campeche Bank the gradients are always offshore, being stronger in July and weaker in October–November. In the section at 95.5°W, on the LATEX shelf, there is a second maximum in May–June, as is observed in the Galveston tide gauge data (Figure 14).

5. Conclusions

[37] With regard to its circulation, the western shelf of the GoM can be divided in three regions: the TAVE shelf, the LATEX shelf, and the western Campeche Bank. Over the TAVE shelf, between 26°N and 19°N, the currents run southward from September to March and northward from May to August, reaching monthly mean speed of 0.70 m s^{-1}; the transition periods are from late March to April and from late August to September. During the fall and winter, low-salinity water from the Mississippi and Atchafalaya rivers is advected across the LATEX shelf to the TAVE shelf, developing fronts along the outer shelf or the shelf break. During the summer season, water from the TAVE shelf is advected onto the LATEX shelf. On the western Campeche Bank, the low-frequency circulation is upcoast throughout the year. On the LATEX shelf, most of the year there is a cyclonic circulation, with a strong coastal current along the inner shelf and a weaker broad current over the

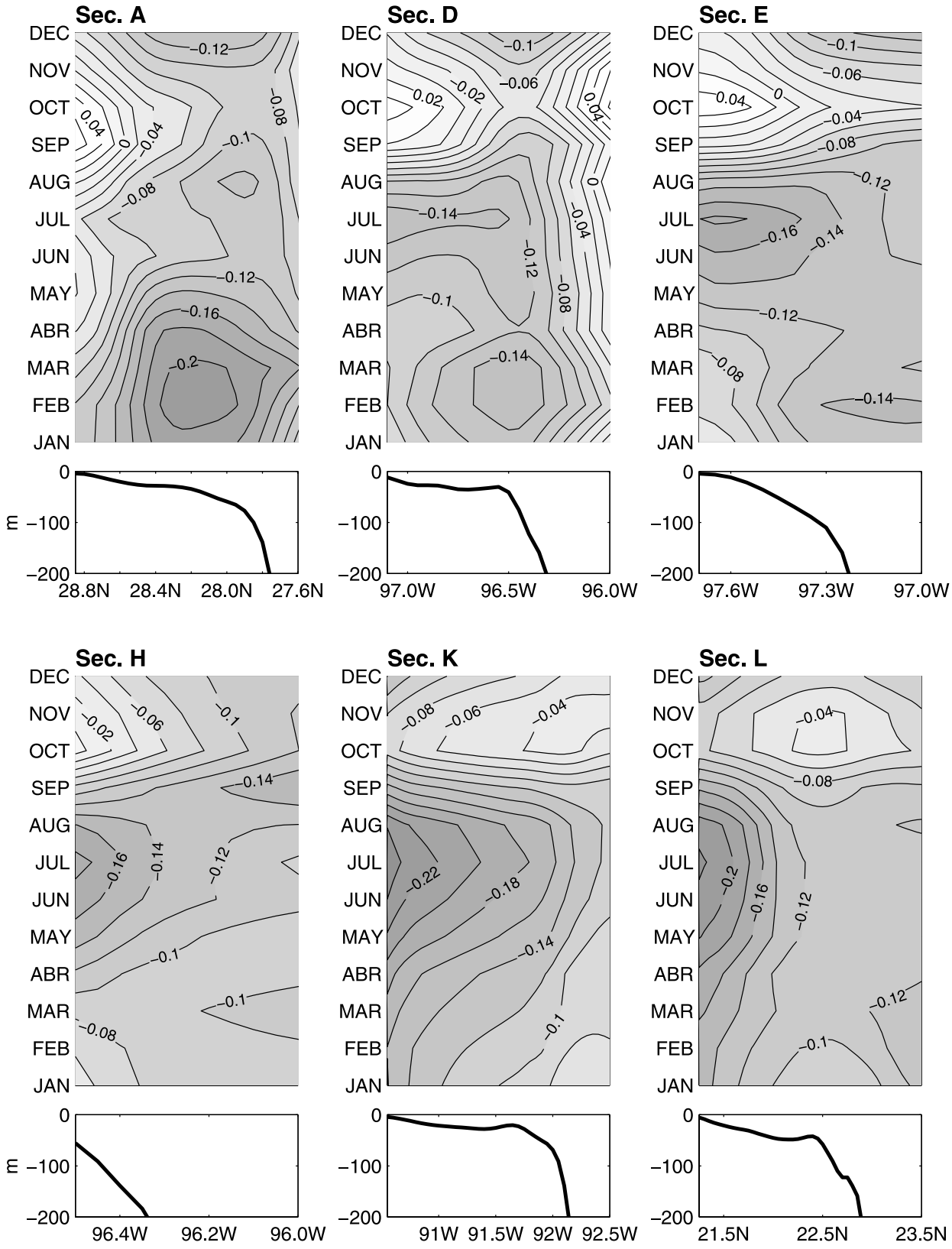

Figure 14. Model monthly mean sea surface height (m) at the sections indicated with corresponding letters in Figure 1. (bottom) The bathymetry of each section.

outer shelf. The results from the model simulations show a stronger outer shelf current in April and May when there is a convergence in the southern Texas shelf that feeds the current. In summer, the currents on the LATEX shelf are eastward.

[38] At the seasonal frequency, the main forcing of the circulation on the western shelf of the gulf is the ACWSC. Its pattern is similar to the local ocean circulation throughout the year. Over the TAVE shelf, the ACWSC is southward from September to March and northward from April to August, as is the along shore current. Over the LATEX shelf the ACWSC is always downcoast, except for the summer months when it is very weak and sometimes reverses, and on the western Campeche Bank is upcoast throughout the year. The correlation between the ACWSC and the along shore surface currents is high over most of the shelf, except for the convergence zones, supporting the hypothesis that the local wind stress is the main forcing mechanism of the western shelf of the GoM. The larger correlation coefficients are on the TAVE shelf, where the ACWSC is stronger and has greater variability at the seasonal scale.

[39] There are two main confluence regions along the western shelf of the GoM: one in the northwest, around 26.5°N, mainly observed from April to August, and the other in the southernmost part of the Bay of Campeche, between 93°W and 95.5°W, observed from September to March. The cause of the confluence of the shelf currents is the convergence of the ACWSC, due to the combination of the concave shape of the western gulf and the wind direction. The main consequence of the confluence is the generation of offshore currents, which are notorious in satellite images because these currents are often associated with waters of high chlorophyll *a* content and contrasting temperature. Although it has been observed that offshore currents are associated with episodic processes, here it is found that these events have a seasonal modulation.

[40] The offshore Ekman transport associated with the upcoast ACWSC favors upwelling during the spring and summer on the TAVE shelf. During the fall and winter the inshore surface Ekman transport favors the downwelling on the inner shelf and the confinement of the low-salinity water to the coast.

[41] **Acknowledgments.** This project was funded by the ONR sponsored Distributed Marine Environment Forecast System, the Office of Naval Research Secretary of the Navy grant awarded to James J. O'Brien, and the NASA Office of Earth Science. Simulations were performed on the IBM SPs at the Florida State University and the Naval Oceanographic Office. Computer time was provided by the DoD High Performance Computing Modernization Office, and by the FSU School of Computational Science and Information Technology. We would like to thank Wilton Sturges and Rosario Romero-Centeno, who made important comments that improved this study. The authors wish to thank reviewer Alexis Lugo-Fernández and one anonymous reviewer for their valuable suggestions. Special thanks to Paul Martin from Stennis Space Center NRL for helping with the implementation of the GoM numerical simulation, to Luis Soto from ICML-UNAM who provided the hydrographic data from the PROBMEX and OGMEX projects, and to Carlos Illescas and Ranulfo Rodriguez who processed them for this study. Juan I. González from CICESE kindly provided the monthly mean tide gauge data. We thank Alex Lee for his contributions to the analysis of the sea level data. The authors would like to thank the SeaWiFS Project (Code 970.2) and the Distributed Active Archive Center (Code 902) at the Goddard Space Flight Center, Greenbelt, MD 20771, for the production and distribution of the data. These activities are sponsored by NASA's Mission to Planet Earth Program.

References

Biggs, D. C., and F. E. Müller-Karger, Ship and satellite observations of chlorophyll stocks in interacting cyclone-anticyclone eddy pairs in the western gulf of Mexico, *J. Geophys. Res.*, *99*, 7371–7384, 1994.

Blaha, J., and W. Sturges, Evidence for wind-forced circulation in the Gulf of Mexico, *J. Mar. Res.*, *39*, 711–734, 1981.

Blumberg, A. F., and G. L. Mellor, A description of a three-dimensional coastal ocean circulation model, in *Three-Dimensional Coastal Ocean Models, Coastal Estuarine Stud.*, vol. 4, edited by N. Heaps, pp. 1–16, AGU, Washington, D. C., 1987.

Boicourt, W. C., W. J. Wiseman Jr., Valle-A. Levinson, and L. P. Atkinson, Continental shelf of the southeastern United States and the Gulf of Mexico: In the shadow of the western boundary current, in *The Sea*, vol. 11, edited by A. R. Robinson and K. H. Brink, pp. 135–182, John Wiley, Hoboken N. J., 1998.

Brooks, D. A., and R. V. Legeckis, A ship and satellite view of hydrographic features in the western Gulf of Mexico, *J. Geophys. Res.*, *87*, 4195–4206, 1982.

Cho, K., R. O. Reid, and W. D. Nowlin Jr., Objectively mapped stream function fields on the Texas-Louisiana shelf based on 32 months of moored current meter data, *J. Geophys. Res.*, *103*, 10,377–10,390, 1998.

Cochrane, J. D., and F. J. Kelly, Low-frequency circulation on the Texas-Louisiana continental shelf, *J. Geophys. Res.*, *91*, 10,645–10,659, 1986.

DaSilva, A., A. C. Young, and S. Levitus, *Atlas of Surface Marine Data 1994,* vol. 1, *Algorithms and Procedures, NOAA Atlas NESDIS,* vol. 6, Natl. Oceanic and Atmos. Admin., Silver Spring, Md., 1994.

Elliott, B. A., Anticyclonic rings in the Gulf of Mexico, *J. Phys. Oceanogr.*, *12*, 1292–1309, 1982.

Fox, D. N., W. J. Teague, C. N. Barron, M. R. Carnes, and C. M. Lee, The Modular Ocean Data Assimilation System (MODAS), *J. Atmos. Oceanic Technol.*, *19*, 240–252, 2001.

Garvin, R. W., Fresh water delivery to the continental shelf and subsequent mixing: An observational study, *J. Geophys. Res.*, *106*, 27,087–27,101, 2001.

González, J. I., J. Ochoa, and P. Ripa, Variación estacional del nivel del mar en el Golfo de México y Mar Caribe, *Geos*, *17*, 168–171, 1997.

Gordon, A., Circulation of the Caribbean Sea, *J. Geophys. Res*, *72*, 6207–6223, 1967.

Greatbatch, R. J., A note on the representation of steric sea level in models that conserve volume rather than mass, *J. Geophys. Res.*, *99*, 12,767–12,771, 1994.

Gutiérrez de Velasco, G., S. Shull, P. J. Harvey, and N. A. Bray, Gulf of Mexico experiment: Meteorological, moored instrument, and sea level observations, in *Data Report 1: August 1990 to July 1991, SIO Ref. 92-26*, 44 pp., Scripps Inst. of Oceanogr., Univ. of Calif., San Diego, 1992.

Gutiérrez de Velasco, G., S. Shull. P. J. Harvey, and N. A. Bray, Gulf of Mexico experiment: Meteorological, moored instrument, and sea level observations, in *Data Report 2: August 1991 to July 1992, SIO Ref. 93-31*, 36 pp., Scripps Inst. of Oceanogr., Univ. of Calif., San Diego, 1993.

Li, Y., W. D. Nowlin Jr., and R. O. Reid, Spatial-scale analysis of hydrographic data over the Texas-Louisiana continental shelf, *J. Geophys. Res.*, *101*, 20,595–20,605, 1996.

Li, Y., W. D. Nowlin Jr., and R. O. Reid, Mean hydrographic fields and their interannual variability over the Texas-Louisiana continental shelf in spring, summer, and fall, *J. Geophys. Res.*, *102*, 1027–1049, 1997.

Lugo-Fernández, A., K. J. Desalrzes, J. M. Price, G. S. Boland, and M. V. Morin, Inferring probable dispersal of Flower Garden Banks coral larvae (Gulf of Mexico) using observed and simulated drifter trajectories, *Cont. Shelf Res.*, *21*, 47–67, 2001.

Martin, P., A description of the Navy Coastal Ocean Model version 1.0, *NRL Rep. NRL/FR/7322-00,9962*, 39 pp., Nav. Res. Lab., Stennis Space Center, Miss., 2000.

Mellor, G. L., and T. Ezer, Sea level variations induced by heating and cooling: An evaluation of the Boussinesq approximation in ocean models, *J. Geophys. Res.*, *100*, 20,565–20,577, 1995.

Merino, M., Upwelling on the Yucatan shelf: Hydrographic evidence, *J. Mar. Syst.*, *13*, 101–121, 1997.

Merrell, W. J., Jr., and J. M. Morrison, On the circulation of the western Gulf of Mexico with observations from April 1978, *J. Geophys. Res.*, *86*, 4181–4185, 1981.

Merrell, W. J., Jr., and A. M. Vázquez, Observations of changing mesoscale circulation patterns in the western Gulf of Mexico, *J. Geophys. Res.*, *88*, 7721–7723, 1983.

Monreal, M. A., D. A. Salas, A. R. Padilla, and M. A. Alatorre, Hydrography and estimation of density currents in the southern part of the Bay of Campeche, Mexico, *Cienc. Mar.*, *18*, 115–133, 1992.

Morey, S. L., P. J. Martin, J. J. O'Brien, A. A. Wallcraft, and J. Zavala-Hidalgo, Export pathways for river discharged fresh water in the northern Gulf of Mexico, *J. Geophys. Res.*, *108*(C10), 3303, doi:10.1029/2002JC001674, 2003a.

Morey, S. L., W. Schroeder, J. J. O'Brien, and J. Zavala-Hidalgo, The annual riverine influence in the eastern Gulf of Mexico, *Geophys. Res. Lett.*, *30*(16), 1867, doi:10.1029/2003GL017348, 2003b.

Müller-Karger, F. E., J. J. Walsh, R. H. Evans, and M. B. Meyers, On the seasonal phytoplankton concentration and sea surface temperature cycles on the Gulf of Mexico as determined by satellites, *J. Geophys. Res.*, *96*, 12,645–12,665, 1991.

National Oceanic and Atmospheric Administration, *World Ocean Atlas 1994* [CD-ROM NODC-43], Natl. Oceanogr. Data Cent., Washington, D. C., 1994.

Nowlin, W. D., Jr., A. E. Jochens, R. O. Reid, and S. F. DiMarco, Texas-Louisiana Shelf circulation and transport processes study: Synthesis report, vol. I, Technical report, *OCS Stud. MMS 98-0035*, 502 pp., U. S. Dep. of the Inter., Mineral. Manage. Serv., Gulf of Mex. OCS Reg., New Orleans, La., 1998.

Nowlin, W. D., Jr., A. E. Jochens, S. F. DiMarco, R. O. Reid, and M. K. Howard, Deepwater physical oceanography reanalysis and synthesis of historical data: Synthesis report, *OCS Stud. MMS 2001-064*, 528 pp., U. S. Dep. of the Inter., Mineral. Manage. Serv., Gulf of Mex. OCS Reg., New Orleans, La., 2001.

Ochoa, J., J. Sheinbaum, A. Badan, J. Candela, and D. Wilson, Geostrophy via potential vorticity inversion in the Yucatan Channel, *J. Mar. Res.*, *59*, 725–747, 2001.

Oey, L.-Y., Eddy and wind-forced shelf circulation, *J. Geophys. Res.*, *100*, 8621–8637, 1995.

Roemmich, D., Circulation of the Caribbean Sea: A well-resolved inverse problem, *J. Geophys. Res.*, *86*, 7993–8005, 1981.

Sheinbaum, J., J. Candela, A. Badan, and J. Ochoa, Flow structure and transport in the Yucatan Channel, *Geophys. Res. Lett.*, *29*(3), 1040, doi:10.1029/2001GL013990, 2002.

Soto, L. A., and E. Escobar, Coupling mechanisms related to benthic production in the SW Gulf of Mexico, in *Biology and Ecology of Shallow Coastal Waters*, edited by A. Eleftheriou, A. D. Ansell, and J. Smith, pp. 233–242, Olsen and Olsen, Fredensborg, Denmark, 1995.

Sturges, W., The annual cycle of the western boundary current in the Gulf of Mexico, *J. Geophys. Res.*, *98*, 18,053–18,068, 1993.

Sturges, W., and J. P. Blaha, A western boundary current in the Gulf of Mexico, *Science*, *92*, 367–369, 1976.

Sturges, W., and R. Leben, Frequency of ring separations from the Loop Current in the Gulf of Mexico: A revised estimate, *J. Phys. Oceanogr.*, *30*, 1814–1819, 2000.

Vázquez, A. M., Bay of Campeche cyclone, Ph. D. thesis, Tex. A&M Univ., College Station, 1993.

Vidal, V. M. V., F. V. Vidal, and J. M. Pérez-Molero, *Atlas Oceanográfico del Golfo de México,* vol. 1, 415 pp., Inst. de Invest. Electr., Cuernavaca, México, 1988.

Vidal, V. M. V., F. V. Vidal, and J. M. Pérez-Molero, *Atlas Oceanográfico del Golfo de México*, vol. 2, 707 pp., Inst. de Invest. Electr., Cuernavaca, México, 1990.

Vidal, V. M. V., F. V. Vidal, and J. M. Pérez-Molero, Baroclinic flows, transports, and kinematic properties in a cyclonic-anticyclonic-cyclonic ring triad in the Gulf of Mexico, *J. Geophys. Res.*, *99*, 7571–7597, 1994a.

Vidal, V. M. V., F. V. Vidal, A. F. Hernández, E. Meza, and L. Zambrano, *Atlas Oceanográfico del Golfo de México*, vol. 3, 586 pp., Inst. de Invest. Electr., Cuernavaca, México, 1994b.

Vukovich, F. M., On the formation of elongated cold perturbations off the Dry Tortugas, *J. Phys. Oceanogr.*, *18*, 1051–1059, 1988a.

Vukovich, F. M., Loop current boundary variations, *J. Geophys. Res.*, *93*, 15,585–15,891, 1988b.

Weatherly, G., N. Wienders, and R. Ahrkema, Temperature inversions in the open Gulf of Mexico, *J. Geophys. Res.*, *108*(C6), 3177, doi:10.1029/2002JC001680, 2003.

Walker, N. D., O. K. Huh, L. J. Rouse Jr., and S. P. Murray, Evolution and structure of a costal squirt off the Mississippi River delta: Northern Gulf of Mexico, *J. Geophys. Res.*, *101*, 20,643–20,655, 1996.

Zavala-Hidalgo, J., A. Pares-Sierra, and J. Ochoa, Seasonal variability of the temperature and heat fluxes in the Gulf of México, *Atmosfera*, *15*, 81–104, 2002.

S. L. Morey and J. J. O'Brien, Center for Ocean-Atmospheric Prediction Studies, Florida State University, Tallahassee, FL 32306-2840, USA.

J. Zavala-Hidalgo, Centro de Ciencias de la Atmósfera, Universidad Nacional Autónoma de México, Ciudad Universitaria 04510 Cd. México, México. (jzavala@atmosfera.unam.mx)